

Investigating the Mechanical Behaviour of Magnesium Alloy under Conventional Turning Process

Deepak¹, Rajender Kumar^{2*}, Puneet Katyal³

^{1,3}Department of Mechanical Engineering, Guru Jambheshwar University of Science & Technology, Hisar

²Department of Basic Engineering, Chaudhary Charan Singh Haryana Agricultural University, Hisar, India-125001

*Email: rksingh@hau.ac.in, *ORCID- 0000-0003-2907-791X, Scopus Author ID 57220595867

Abstract:- Magnesium alloys are mainly used in various architectural applications because of their lightweight, high strength, and excellent damping features. However, in-flammability is constraint in machining the alloy. Conventional turning operation under machining has been performed on AZ91 Mg alloy in current study, to find out response characteristics such as surface roughness (SR), metal removal rate (MRR) and chip morphology. L9 orthogonal array was considered to study the effect of turning process parameters such as depth of cut (D), feed rate (F), and cutting speed (V). The results observed that the turning parameters variation influences the MRR and surface integrity of AZ91 Mg alloy inclusive of chip morphology. Scanning electron microscopy was evaluated to correlate the effect of turning parameters on the machining performance. All process parameters have a synergistic influence on surface roughness. The cutting speed exerts a significant influence on the formation of chip types. As per the results, the most influencing characteristics with the use of the multi-objective optimization grey relational analysis are the cutting speed with reducing SR and maximizing MRR for the low down the degradation behavior of the Mg alloys. The GRA technique suggests that the optimal parametric setting for turning of AZ91 is V1(1500 rpm)-F3(250 mm/min)-D3(0.75 mm) for minimum SR and maximum MRR. This configuration is recommended to ensure the mechanical integrity and degrading behaviour for In-vitro studies.

Keywords: Mg alloys, Turning, GRA, Chip morphology, MRR, Roughness

1. Introduction

Magnesium ion is a biological products metabolite that exists in bones that is absorbed daily in quantities that vary from 250 to 300 mg [1,2]. Over the past few years, the rising potential of the use of magnesium and magnesium alloys in biomaterials has posed a significant challenge for researchers and industry professionals. Utilizing biomaterials that are compatible with bone regeneration and possesses high mechanical, wear, and corrosion resistance along with favorable biocompatibility is essential [3]. Magnesium and its alloys have the potential for biodegradable implants due to their light weight and high strength relative to its density, as well as a low value of elastic modulus (45GPa) and mechanical properties that are comparable to natural human bone (10-30GPa) [4,5]. Several different biodegradable magnesium-based alloys are being developed for the placement of magnesium inside the human and animal body with these properties. Even though, Mg alloys possess drawbacks including H₂ evolution in physiological conditions, contributes to a rapid decline in mechanical strength and the development of toxicity at the site of implantation that impedes the expanding

potential of Mg in the biomedical area [6-8]. When a product fails, it usually begins at the surface, regardless of the reason- wear, corrosion or crack propagation [9]. To overcome the corrosion rate, the degradation behavior needs to study that is depends on the surface integrity. Surface roughness (SR) affects the mould ability to adhere well, which is important for producing medical devices [10]. The characteristics of the surface produced, including surface texture and conditions below the surface, has a significant impact on the functional performance of each devices prepared by material removal process especially machining operations [11]. Magnesium alloys have a low density, which makes them more suitable for machining due to their advantages of reduced power consumption, extended tool life, and improved surface quality. Therefore, the conventional machining operations must be prioritized in the processing of biomedical implants based on Mg-alloys [12]. The conventional turning processes with cutting speed, feed rate and depth of cut have significant effect on the removal rate and surface integrity. Higher speeds with lower feeds and depth of cut will result in an improved surface quality in case of AM series Mg alloys studied by [13]. Vasu et al. [14] optimized the response characteristic of AZ91 Mg alloy machining with uncoated carbide cutting tools under dry machining conditions using grey relational analysis. The carbide tool with high cutting-edge angle had higher surface roughness irrespective of cutting speed and feed rates. Danish et al. [15] examined the processing of Mg alloys using different environment-friendly cooling methods and observed low feed rate with speed range 50-150 m/min for optimal surface finish with high material removal rate (MRR). Viswanathan et al. [16] used a grey-based Taguchi approach under dry condition to analyze material removal rate, cutting force, tool flank wear, and SR when turning magnesium alloy with PVD-coated carbide insert. Low cutting speed generated small fragmented chips during turning of Mg alloy. Asal [17] studied the impact of cutting variables on surface roughness in AZ31 magnesium alloys with Taguchi's L_9 model and observed feed rate has more impact on SR followed by cutting speed.

There are numerous experimental studies that focus on turning with Mg alloys with specific conditions of depth studies, coolant, modelling and forecasting, cutting tools, chip formation inclusive different metallic materials referred to surface roughness [18-21]. However, there is a significant paucity of research work in the field of optimizing turning parameters for biodegradable Mg alloy. Consequently, in the present study, using Taguchi's L_9 orthogonal array (OA), the turning process parameters for MRR and SR, with chip morphology of AZ91 magnesium alloy were analysed to address the research gap. The GRA technique was implemented to consolidate multiple responses into a single response in order to address multiple performance characteristic with an objective of increase MRR and reduce SR. The process parameters have also been discussed for surface topography of machined surfaces.

2. Experimental details and methodology

In the study, AZ91 Mg alloy plate having composition as per given in Table 1 is used. The plate with dimension $100 \times 100 \times 30$ mm has been initially machined to create smoother surface for preparing the samples. The specimen dimension measuring $10 \times 10 \times 2$ mm cuts from parent material for testing composition through scanning electron microscope (SEM). The SEM (JSM-7610F Plus) uses high resolution imaging of the area being tested to find the precise chemical makeup of the material sample. The chemical composition observed of Mg alloy through SEM analysis is given through Fig. 1 and illustrated in Table 1.

On a CNC Turning lathe (Hytech automation, model SLT-100 CNC, fitted with a Siemens advance controller)

with very precise tolerances, the turning tests were performed without the use of cooling techniques at the machining zone. Specimen of size 30 mm lengths with diameter 27.5 mm was prepared with WEDM processes. Then, the experiments were performed with cutting speed (1500, 2000 and 2500 rpm), feed rates (150, 200 and 250 mm/min), and depth of cut (0.25, 0.5 and 0.75mm) under dry condition after polishing as shown in Table 2. MRR and SR response parameters were analyzed with chips evolution after each experiment. L_9 orthogonal array is used for experiments with Minitab for analysis and grey relational analysis (GRA) technique is adopted for multi response optimization. Surface roughness tester (Mitutoyo, SJ410) is used for measuring roughness by taking average value on the turning surface. A stereomicroscope was used with scale for the measurement of chip thickness (average in μm) and length (mm). The process flow of the experiment is shown in Fig. 2.

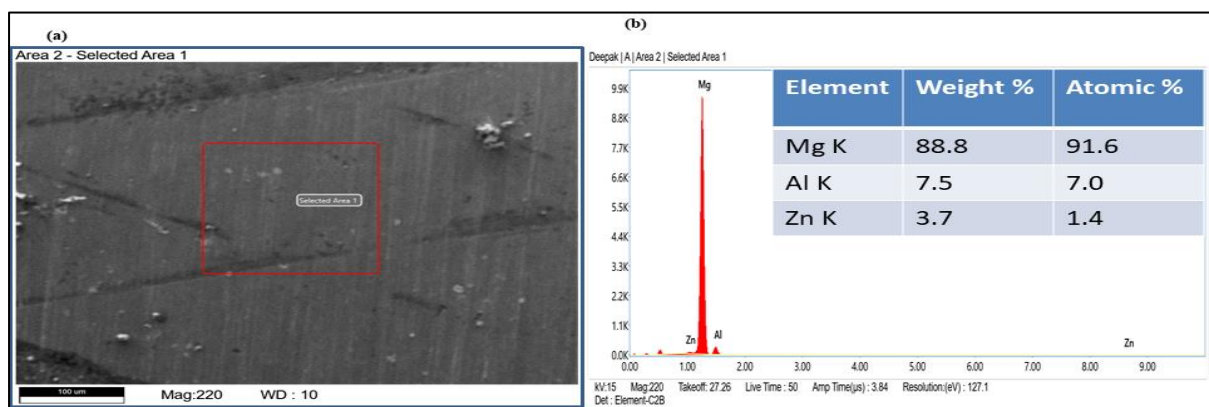


Fig. 1. (a) SEM and (b) EDS analysis of AZ91 alloy of the machined specimen

Table 1

The chemical composition of the AZ91Mg alloy.

Element	Mg	Zn	Al
Wt. %	91.6	1.4	7.0

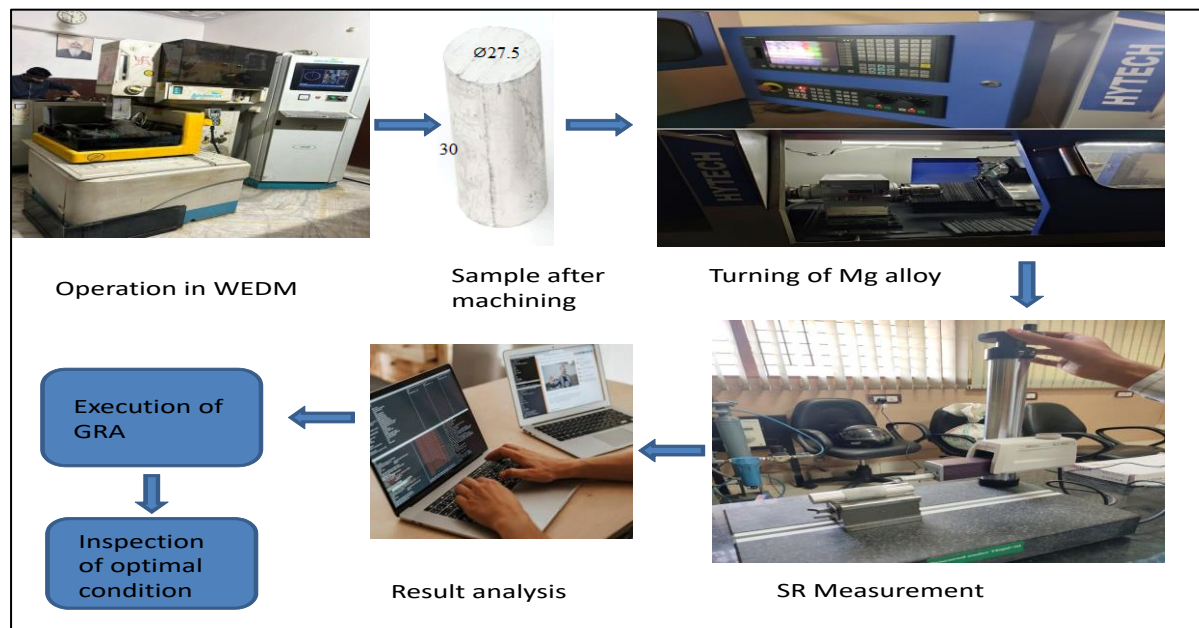


Fig. 2. Process flow of the experiment.

Table 2

Turning process parameters with level.

Cutting parameters	Symbol	Units	Level		
			Level 1	Level 2	Level 3
Cutting speed	V	RPM	1500	2000	2500
Depth of cut	D	mm	0.25	0.5	0.75
Feed rate	F	mm/min	150	200	250

3. Result and Discussion

Using L_9 orthogonal array, the values of MRR and SR for each parametric combination are provided in Table 3. Analysis of Variance (ANOVA) was considered for the percentage contribution and significant values with the use of Minitab-21 version. The process parameter's effect with the level of operations on response parameters are illustrated in the following sections.

Table 3

Experimental design using L_9 OA layout using Taguchi method

Process parameters				Response Parameters	
Exp. No.	Cutting speed (rpm)	Feed rate (mm/min)	Depth of cut (mm)	Surface roughness (R_a), μm	MRR mm^3/min
1	1500	150	0.25	1.782	3254.5
2	1500	200	0.50	2.187	7537.9
3	1500	250	0.75	2.675	15126.8
4	2000	150	0.50	0.564	1231.3
5	2000	200	0.75	1.599	11507.9
6	2000	250	0.25	2.034	4627.2
7	2500	150	0.75	1.244	8103.6

8	2500	200	0.25	1.629	4280.4
9	2500	250	0.50	2.136	8756.4

3.1 Material Removal Rate for single response optimization

The effect of process parameter on MRR has shown in Fig. 3. It reveals that MRR value first decreases with the increase of speed from 1500 to 2000rpm, due to cutting forces involvement with surface hardening, and then increases with the increase in speed from 2000 to 2500 rpm because of thermal softening effect. By increasing both feed rate and depth of cut values from 150 to 250 mm/min and 0.25 to 0.75 mm respectively, an apparent rise in MRR is consistently observed. With the increase in cutting speed per unit area, chip thickness increases, and there is a corresponding increase in the amount of material sheared by the tool. When depth of cut increases, the material's shearing area also increases, resulting in thicker chips, higher thermal stresses and cutting forces [12]. This ultimately leads to a higher MRR. When comparing CS, it is observed that the influences of feed rate and depth of cut are more prominent in the turning process of AZ91 Mg Alloys.

In order to investigate the effect of process parameters, an analysis of variance (ANOVA) was chosen, employing a 5% significance level on the response [22]. Notably, Table 4 indicates that D has the highest Delta value (max-min; D= 7525), indicating that D is the most influential factor. In accordance with Table 5, all process parameters have a substantial impact on MRR, except for cutting speed. Among the process parameters, F contributes 29.10% and D contributes 61.40% to the MRR, making them the most significant contributors. Taguchi analysis determined that the maximum MRR value for single response optimization is achieved with the following parameter settings: V₁: 1500 rpm; F₃: 250 mm/min; and D₃: 0.75 mm (as shown in Fig. 3). The anticipated Signal-to-Noise (S/N) ratio is 86.1813 and Mean value is 15405.7 for the setting.

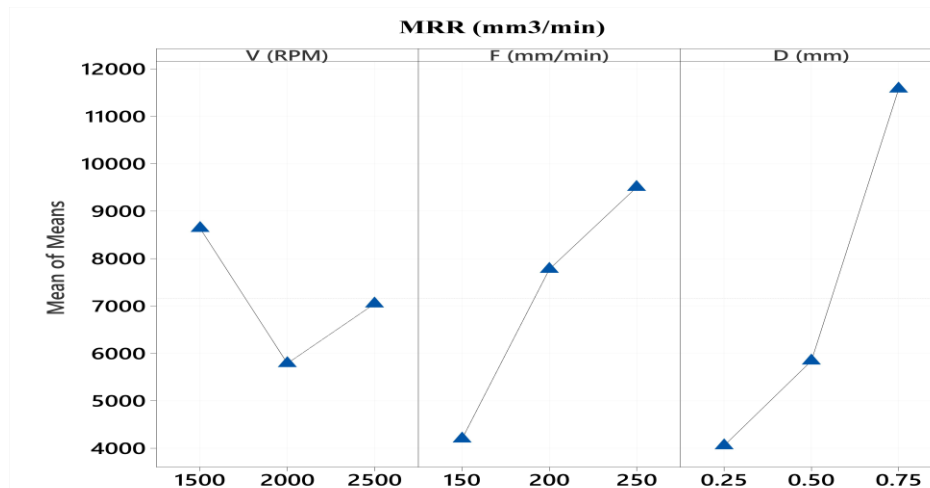


Fig. 3. Main effects plot for MRR.

Table 4

Response Table for Means.

Level	V (rpm)	F (mm/min)	D (mm)
1	8640	4196	4054
2	5789	7775	5842
3	7047	9503	11579

Delta	2851	5307	7525
Rank	3	2	1

Table 5

Analysis of Variance for MRR.

Factor	D.F	SS	Contribution	MS	F-Value	P-Value
V (rpm)	2	12247821	8.11%	6123911	5.80	0.147
F (mm/min)	2	43959227	29.10%	21979614	20.83	0.046
D (mm)	2	92747664	61.40%	46373832	43.94	0.022
Error	2	2110670	1.40%	1055335		
Total	8	151065383	100.00%			

S: 1027.29; R-sq.: 98.60%; R-sq(adj): 94.41%

Regression Equation

MRR (mm³/min)= 7158 + 1481 V (rpm)_1500 - 1370 V (rpm)_2000 - 112 V (rpm)_2500- 2962 F (mm/min)_150
+ 617 F (mm/min)_200 + 2345 F (mm/min)_250- 3104 D (mm)_0.25 - 1317 D (mm)_0.50 + 4421 D (mm)_0.75

3.2 Surface Roughness for single response optimization

Surface integrity is important for performance forecasting of Mg-alloy components because surface imperfections greatly enhance corrosion location susceptibility [23]. Material composition, cutting parameters and machining environment play a substantial role in significantly influencing the surface roughness (SR). Fig. 4 shows that SR decreases as cutting speed increases from 1500 to 2000 rpm, and then it increases as speed increases from 2000 to 2500 rpm. High CS values lead to increased heat generation at the work surface, which subsequently causes thermal degradation of the material and a decrease in cutting forces. As a result, SR reduces as CS increases. Later on, the cutting at a higher speed and in dry conditions causes the temperature to rise because of heat buildup [24]. Tool face adhesive chipped as a result of increased friction as well that result in increase in SR.

Feed rate is the vital important variable that determines SR, followed by cutting speed and depth of cut. From Fig. 4, SR decreases continuously with the increase in FR from 150 rev/mm to 250 rev/mm. Increased feed rates generate cracking and vibrations, which have a negative impact on surface roughness. Additionally, increased feed rates appear to cause the chips to adhere to the rake face, leading to a decrease in surface quality. The role of feed is crucial in determining the precision of machined surfaces in magnesium alloys [25]. The thermal softening effect causes the surface roughness to decrease as the depth of cut increases from 0.25 mm to 0.50 mm. However, the work required to cut metal increases as the depth of cut (D) increases from 0.50 mm to 1.0 mm, resulting in an increase in roughness due to the formation of a built-up edge on the cutting tool [26].

Using ANOVA presented in Table 7, it can be deduced that the F parameter is highly significant factors (P-Value ≤ 0.05) that influences SR, contributing 59.62% followed by cutting speed with 34.80% as also observed by Table 6. Based on Taguchi analysis, the minimum SR value for single response optimization is obtained with the following parameter settings: V₂: 2000 rpm; F₃: 150 mm/min; and D₂: 0.50 mm. The expected Signal-to-Noise (S/N) ratio is -8.76472, and mean value is 0.350733 for the given configuration through minitab-21 software.

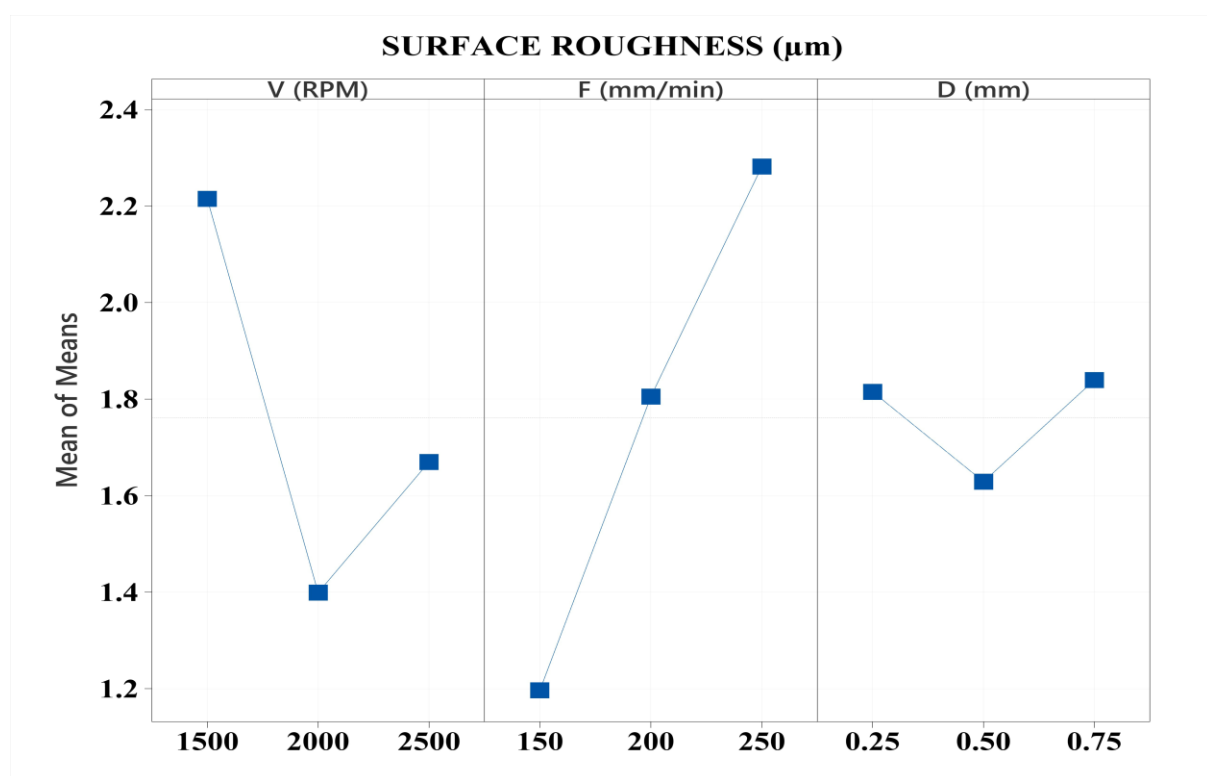


Fig. 4. Main effects plot for SR.

Table 6 Response Table for Means (SR).

Level	V (rpm)	F (mm/min)	D (mm)
1	2.215	1.197	1.815
2	1.399	1.805	1.629
3	1.670	2.282	1.839
Delta	0.816	1.085	0.210
Rank	2	1	3

Table 7 Analysis of Variance for SR.

Source	DF	Seq SS	Adj MS	F-Value	P-Value	Contribution
V (RPM)	2	1.03560	0.51780	11.94	0.077	34.80%
F (mm/min)	2	1.77451	0.88725	20.47	0.047	59.62%
D (mm)	2	0.07943	0.03971	0.92	0.522	2.67%
Error	2	0.08670	0.04335			2.91%
Total	8	2.97623				100.00%

S: 0.208208; R-sq.: 97.09%; R-sq(adj): 88.35%

Regression Equation

$$\begin{aligned} \text{SR } (\mu\text{m}) = & 1.7611 + 0.4536 \text{ V (RPM)}_{1500} - 0.3621 \text{ V (RPM)}_{2000} - 0.0914 \text{ V (RPM)}_{2500} \\ & 0.5644 \text{ F (mm/min)}_{150} + 0.0439 \text{ F (mm/min)}_{200} + 0.5206 \text{ F (mm/min)}_{250} \\ & + 0.0539 \text{ D (mm)}_{0.25} - 0.1321 \text{ D (mm)}_{0.50} + 0.0782 \text{ D (mm)}_{0.75} \end{aligned}$$

3.3 Effect of Chip Morphology

Machinability of alloys such as titanium and Mg alloys are significantly influenced by the formation of chips. In addition, the thermal behaviour at the interface between the workpiece and the tool is influenced by the morphology of the chip, which has an impact on tool life.

It is imperative to investigate the impact of chip formation on machinability in order to enhance productivity and tool life for Mg based alloys. Fig. 5 lists the several types of chips that were formed at different experimental operating settings. Short chip forms at low cutting speed as shown in Exp. 1. The chips are separated into numerous small, fragmented chips at lower cutting speeds, a phenomenon that is attributed to the rubbing action on the tool's rake-face [12,16]. It appears that the types of chips produced underwent minimal variation as the cutting thickness was altered. In Fig. 5, Exp no 6, 9 show that the chip formation is continuous and long with the increasing speed, feed rate and depth of cut. The heat generated during the turning of magnesium alloy results in chip melting, which in turn causes the chips to adhere to the tool edges. This is due to the fact that the sharpness of chip edges is significantly reduced at lower feed rates in turning. Conversely, the linear speed per unit area of chip thickness increases as the F increases, and the shearing area of the material increases as the depth increases [12]. Consequently, the chip thickness and carrying strain hardening effect are both increased. Residual stresses on the machined surface are caused by material shrinkage at the grain boundaries after chips are removed. Micro-cracks form on the machined surface due to these leftover stresses that are susceptible to degradation [12,22] as shown in Fig. 7 (a and b) though SEM and EDS analysis of AZ91 Mg-alloy specimen after turning operations. A higher chip thickness corresponds with a higher rate of heat generation, which in turn increases the possibility of a lesser tool life. Fig. 6 illustrates the characteristics of the chips in accordance with the ISO 3685-1977(E) standard (ISO 1993) [27], which are significantly comparable to the results achieved. Chips adhere to the tool face as a result of the cutting tool's friction, which has a direct effect on the surface morphology and tool life [24]. Thus, chip morphology can be used to compare cutting forces, tool wear, and machined surface quality for various processes attributes [28]. Therefore, the efficacy of the feed rate in chip formation has been observed to be inadequate. Consequently, the cutting speed is the primary factor determining chip formation. Long chips compromise the material's surface roughness and put operators' health at threat, whilst short chips deliver higher worker or operator security.



Fig. 5. Chip formation during experiments at different parametric settings.

1 RIBBON CHIPS*	2 TUBULAR CHIPS*	3 SPIRAL CHIPS	4 WASHER-TYPE HELICAL CHIPS*	5 CONICAL HELICAL CHIPS*	6 ARC CHIPS**	7 ELEMENTAL CHIPS	8 NEEDLE CHIPS
1.1 Long	2.1 Long	3.1 Flat	4.1 Long	5.1 Long	6.1 Connected		
1.2 Short	2.2 Short	3.2 Conical	4.2 Short	5.2 Short	6.2 Loose		
1.3 Snarled	2.3 Snarled		4.3 Snarled	5.3 Snarled			

Fig. 6. Chip formation as per standard ISO 3685-1977 (ISO 1993) [27].

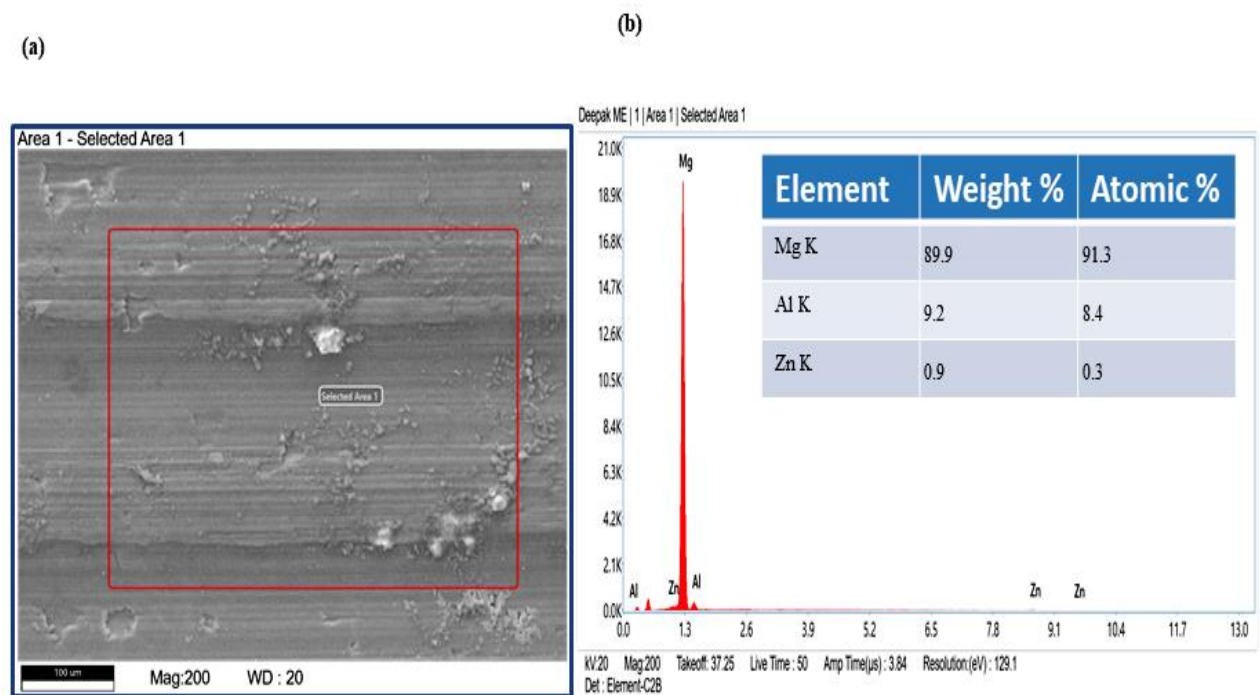


Fig. 7. (a) SEM and (b) EDS analysis of AZ91 Mg-alloy specimen after turning operation.

3.4 Grey relation analysis for multi-response optimization

The current study uses a mathematical approach based on GRA to perform multi-functional optimization. When multiple characteristics are simultaneously optimized for multiple response characteristics, GRA is employed as per the procedure followed by R. Kumar [12,29]. Fig. 8 illustrates the grey relational analysis (GRA) flow sequence. The higher value of GRG recommends the optimal solution to the process variables, and better response parameter as renders in Exp. No 3. Table 8 shows the calculated GRC and GRG. Finding the optimal parameter settings to achieve a greater GRG value, which in turn indicates optimized SR and MRR, is the present objective of the investigation.

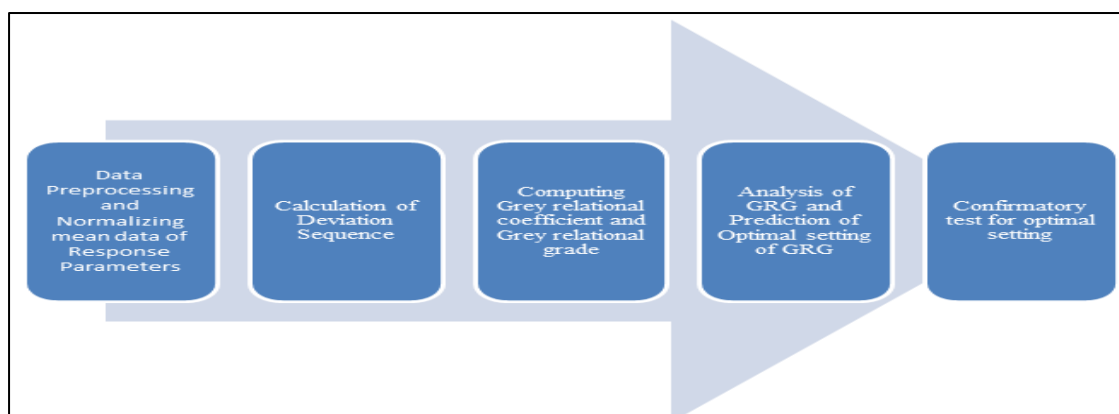


Fig. 8. The flow sequence for Grey Relational Analysis.

Table 8

Data pre-processing and computing GRG.

Exp. Run	Normalization of mean data for response		Deviation sequence		Grey relational coefficient (GRC)		GRG	Rank
	MRR	SR	MRR	SR	MRR	SR		
1	0.39	0.739	0.61	0.26	0.449	0.657	0.553	8
2	0.72	0.871	0.28	0.13	0.643	0.794	0.719	3
3	1.00	1.000	0.00	0.00	1.000	1.000	1.000	1
4	0.00	0.000	1.00	1.00	0.333	0.333	0.333	9
5	0.89	0.669	0.11	0.33	0.821	0.602	0.712	4
6	0.53	0.824	0.47	0.18	0.514	0.740	0.627	5
7	0.75	0.508	0.25	0.49	0.668	0.504	0.586	6
8	0.50	0.681	0.50	0.32	0.498	0.611	0.555	7
9	0.78	0.855	0.22	0.14	0.696	0.776	0.736	2

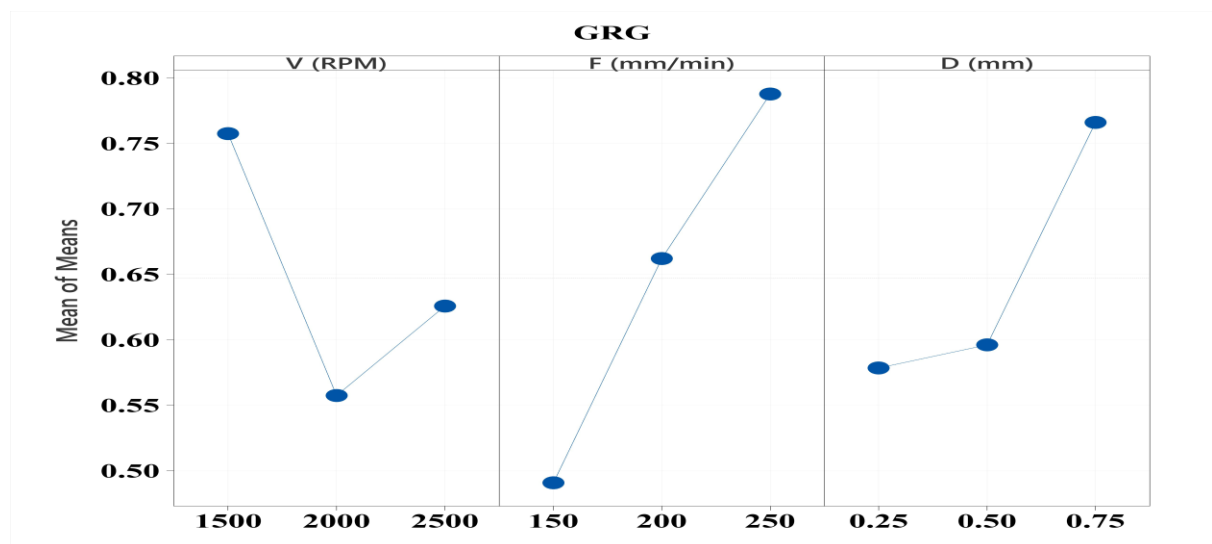


Fig. 9. Effect of grade values (Mean of means) for turning process parameters.

Analysis of variation (ANOVA), a statistical technique, was employed to validate the process parameters that exert a substantial influence on the process response with a confidence level of 95%.

For the purposes of the analysis, the results obtained through multiple iterations were analyzed using the "larger the better" approach. Notably, Table 9 indicates that F has the highest Delta value (max-min; $F = 0.2970$), indicating that F is the most influential factor, followed by V and D, which have a less noticeable effect on the GRG. The parameters that contribute to the GRG calculation are F (50.91%), D (24.60%), and V (23.67%), as shown in ANOVA Table 10. Consequently, the optimum parameter combination is V_1 (1500 rpm)- F_3 (250 mm/min)- D_3 (0.75 mm) as shown in Fig. 9. At the particular setting, the Taguchi approach predicted a grade mean of 101744 and S/N ratio 0.778895 from minitab-21 version.

Table 9 Response Table for Means of GRG.

Level	V (rpm)	F (mm/min)	D (mm)
1	0.7573	0.4907	0.5783

2	0.5573	0.6620	0.5960
3	0.6257	0.7877	0.7660
Delta	0.2000	0.2970	0.1877
Rank	2	1	3

Table 10 Analysis of Variance for GRG.

Factor	D.F	SS	Contribution	MS	F-Value	P-Value
V (rpm)	2	0.062006	23.67%	0.031003	28.67	0.034
F (mm/min)	2	0.133356	50.91%	0.066678	61.66	0.016
D (mm)	2	0.064431	24.60%	0.032215	29.79	0.032
Error	2	0.002163	0.83%	0.001081		
Total	8	0.261956	100.00%			

S: 0.0328853; R-sq.: 99.17%; R-sq(adj): 96.70%

3.5 Computing optimum value for GRG with confirmatory test

The relevant characteristics were included in the ANOVA model to predict the optimal values for GRG. The equation 1 shown below can be used to calculate the estimated GRG at optimal settings.

$$\Psi_{\text{Opt}} = \Psi_m + \sum_{k=1}^n (\Psi_k - \Psi_m) \quad \text{----- Eq.1}$$

Ψ_{Opt} is the optimal grade; Ψ_k is the optimum level means for GRG, Ψ_m is the total mean of GRG; and n is the number of process parameters. If the process parameters are numerous, significant parameters may be taken into account. Here, the values required to predict the optimal GRG are based on three process parameters. The desired grade value is obtained as 1.01740 by utilizing the aforementioned equation.

$$\Psi_{\text{Opt}} (\text{estimated}) = 0.6467 + (0.7573 - 0.6467) + (0.7877 - 0.6467) + (0.7658 - 0.6467) = 1.0174$$

For MRR:

The overall mean $\text{MRR}_\mu = 7158.444 \text{ mm}^3/\text{min}$, so the estimated value of MRR is computed as follows:

$$\text{MRR}_p = (\text{Vm}_1 + \text{Fm}_3 + \text{Dm}_3) - (q-1) \text{MRR}_\mu \quad (\text{where } q = \text{number of process parameters used})$$

$$= (8639.733 + 9503.467 + 11579.43) - 2 * 7158.444 = 15405.74 \text{ mm}^3/\text{min}$$

Similarly for SR: $\text{SR}_p = 2.8134 \mu\text{m}$

The GRG is predicted using the experimental results as per Table 9, which defines the process parameters for each step. Test No. 3 (Table 8) exhibits the highest GRG among the nine experiments using the optimal process set of V_1 - F_3 - D_3 , indicating the best multiple performance characteristics. In order to verify the predicted ideal results using Taguchi-based GRA, the experiments were conducted using an optimal set of parameters i.e. V_1 (1500 rpm)- F_3 (250 mm/min)- D_3 (0.75 mm) and the experimental results obtained are MRR: $15126.8 \text{ mm}^3/\text{min}$ and SR: 2.675 mm that is close to the predicted values given in Table 11.

Table 11 Taguchi optimization based on grey relations confirming the experimental results.

Method	Response	Optimal condition		%age deviation = $\pm(P-E)/P * 100$
		Predicted optimal value (P)	Experimental value (E)	
Multi response optimization	MRR (mm^3/min)	15405.74	15126.8	1.8106

SR (μm)	2.8134	2.675	4.9193
----------------------	--------	-------	--------

4. Conclusion

The present study focuses on the machining of AZ91 magnesium alloy under different cutting circumstances, without the use of lubrication throughout the machining process. Surface roughness, MRR are the response variables taken into account for the current machining process with the impact of chip morphology. The general linear approach is used to optimize the process parameters. The turning procedure of the AZ91 magnesium alloy resulted in the following significant observations.

- Enhancing the cutting speed results in a reduction in MRR and SR. However, increasing the feed rate and depth of cut results in a simultaneous increase in both the MRR and SR. Depth of cut is the most influential parameter for MRR, while the feed rate is most influencing parameter for optimizing the SR in single response optimization. Furthermore, cutting speed is the most influential component in determining chip morphology.
- Chip morphology can be utilized to compare cutting forces, machined surface quality, and tool wear for different process attributes, with short chips recommended.
- Using Taguchi method for single response attributes, the optimized process parameters were found as; for maximum MRR; V_1 : 1500 rpm; F_3 : 250 mm/min; and D_3 : 0.75 mm; for minimum SR; V_2 : 2000 rpm; F_3 : 150 mm/min; and D_2 : 0.50 mm.
- According to Taguchi-based GRA, the optimal configuration for multi-response optimization is V_1 (1500 rpm)- F_3 (250 mm/min)- D_3 (0.75 mm)). F (50.91%), D (24.60%), and V (23.67%), according to analysis of variance on GRA values, are the most significant factors in multi-objective optimization.
- To ascertain the turning method for Mg-alloy implant fabrication, further research can look into the relationship between chip morphology, surface characteristics, fracture density, and mechanical integrity loss.

Funding

The authors declare that there is no source of funding.

Conflict of interest

The authors declare that there are no conflicts of interest.

References

- [1] R. Kumar, P. Katyal, Effects of alloying elements on performance of biodegradable magnesium alloy, Mater. Today Proc. 56 (2022) 2443-2450, <https://doi.org/10.1016/j.matpr.2021.08.233>.
- [2] S. Kumar, P. Katyal, Factors affecting biocompatibility and biodegradation of magnesium based alloys, Mater. Today Proc. 52 (2022) 1092-1107, <https://doi.org/10.1016/j.matpr.2021.10.499>.
- [3] R. Kumar, P. Katyal, K. Kumar, V. Singh, Multiresponse optimization of end milling process parameters on ZE41A Mg alloy using Taguchi and TOPSIS approach, Mater. Today Proc. 56 (2022) 2497-2504, <https://doi.org/10.1016/j.matpr.2021.08.271>.
- [4] T.T.T. Trang, J.H. Zhang, J.H. Kim, A. Zargaran, J.H. Hwang, B.C. Suh, N.J. Kim, Designing a

- magnesium alloy with high strength and high formability, *Nature Nat. Commun.* 9 (1) (2018) 2522, <https://doi.org/10.1038/s41467-018-04981-4>.
- [5] F. Witte, V. Kaese, H. Haferkamp, E. Switzer, A. Meyer-Lindenberg, C.J. Wirth, H. Windhagen, In vivo corrosion of four magnesium alloys and the associated bone response, *Biomaterials* 26 (17) (2005) 3557-3563, <https://doi.org/10.1016/j.biomaterials.2004.09.049>.
- [6] K. Kumar, R.S. Gill, U. Batra, Challenges and opportunities for biodegradable magnesium alloy implants, *Mater. Technol.* 33 (2) (2018) 153-172, <https://doi.org/10.1080/10667857.2017.1377973>.
- [7] M.P. Staiger, A.M. Pietak, J. Huadmai, G. Dias, Magnesium and its alloys as orthopedic biomaterials: a review, *Biomaterials* 27 (9) (2006) 1728-1734, <https://doi.org/10.1016/j.biomaterials.2005.10.003>.
- [8] B.R. Sunil, K.V. Ganesh, P. Pavan, G. Vadapalli, Ch Swarnalatha, P. Swapna, P. Bindukumar, G.P.K. Reddy, Effect of aluminum content on machining characteristics of AZ31 and AZ91 magnesium alloys during drilling, *J. Magnes. Alloy.* 4 (1) (2016) 15-21, <https://doi.org/10.1016/j.jma.2015.10.003>.
- [9] M. Yasir, M. Danish, M. Mia, M.K. Gupta, M. Sarikaya, Investigation into the surface quality and stress corrosion cracking resistance of AISI 316L stainless steel via precision end-milling operation, *Int. J. Adv. Manuf. Technol.* 112 (2021) 1065-1076, <https://doi.org/10.1007/s00170-020-06413-4>.
- [10] C.M. Yousuff, M. Danish, E.T.W. Ho, I.H. Kamal Basha, N.H.B. Hamid, Study on the optimum cutting parameters of an aluminum mold for effective bonding strength of a PDMS microfluidic device, *Micromachines* 8 (8) (2017) 258, <https://doi.org/10.3390/mi8080258>.
- [11] F. Pusavec, H. Hamdi, J. Kopac, I.S. Jawahir, Surface integrity in cryogenic machining of nickel based alloy—Inconel 718, *J. Mater. Process. Technol.* 211 (4) (2011) 773-783, <https://doi.org/10.1016/j.jmatprotec.2010.12.013>.
- [12] R. Kumar, P. Katyal, K. Kumar, N. Sharma, Investigating machining characteristics and degradation rate of biodegradable ZM21 magnesium alloy in end milling process, *Int. J. Lightweight Mater. Manuf.* 5 (1) (2022) 102-12, <https://doi.org/10.1016/j.ijlmm.2021.11.002>.
- [13] S. Dutta, S.K.R. Narala, Optimizing turning parameters in the machining of AM alloy using Taguchi methodology, *Measurement* 169 (2021) 108340, <https://doi.org/10.1016/j.measurement.2020.108340>.
- [14] C. Vasu, A.B. Andhare, R. Dumpala, Multiobjective optimization of performance characteristics in turning of AZ91 Mg alloy using grey relational analysis, *Mater. Today Proc.* 42 (2021) 642-649, <https://doi.org/10.1016/j.matpr.2020.11.049>.
- [15] M. Danish, S. Rubaiee, H. Ijaz, Predictive modelling and multi-objective optimization of surface integrity parameters in sustainable machining processes of magnesium alloy, *Materials* 14 (13) (2021) 3547, <https://doi.org/10.3390/ma14133547>.
- [16] R. Viswanathan, S. Ramesh, S. Maniraj, V. Subburam, Measurement and multi-response optimization of turning parameters for magnesium alloy using hybrid combination of Taguchi-GRA-PCA technique, *Measurement* 159 (2020) 107800, <https://doi.org/10.1016/j.measurement.2020.107800>.
- [17] Ö Asal, Optimization of surface roughness in turning of AZ31 magnesium alloys with Taguchi method. *GUJSA.* 6 (1) (2019) 25-32.
- [18] M. Danish, T.L. Ginta, A.M.A. Rani, D. Carou, J.P. Davim, S. Rubaiee, S. Ghazali, Investigation of surface integrity induced on AZ31C magnesium alloy turned under cryogenic and dry conditions,

- Procedia Manuf. 41 (2019) 476-483, <https://doi.org/10.1016/j.promfg.2019.09.035>.
- [19] S. Tekumalla, M. Ajjarapu, M. Gupta, A novel turning-induced-deformation based technique to process magnesium alloys, *Metals* 9 (8) (2019) 841, <https://doi.org/10.3390/met9080841>.
- [20] B.B. Buldum, A. Şık, A. Akdağlı, M.B. Biçer, K. Aldaş, İ. Özkul, ANN surface roughness prediction of AZ91D magnesium alloys in the turning process, *Mater. Test.* 59 (10) (2017) 916-920, <https://doi.org/10.3139/120.111088>.
- [21] X.H. Guo, L.J. Teng, W. Wang, T.T. Chen, Study on the cutting properties about magnesium alloy when dry turning with kentanium cutting tools, *Adv. Mater. Res.* 102 (2010) 653-657, <https://doi.org/10.4028/www.scientific.net/AMR.102-104.653>.
- [22] R. Kumar, P. Katyal, S. Mandhania, Grey relational analysis based multiresponse optimization for WEDM of ZE41A magnesium alloy, *Int. J. Lightweight Mater. Manuf.* 5 (4) (2022) 543-554, <https://doi.org/10.1016/j.ijlmm.2022.06.003>.
- [23] M.S. Sukumar, P.V. Ramaiah, A. Nagarjuna, Optimization and prediction of parameters in face milling of Al-6061 using Taguchi and ANN approach, *Procedia Eng.* 97 (2014) 365-371, <https://doi.org/10.1016/j.proeng.2014.12.260>.
- [24] S. Dinesh, V. Senthilkumar, P. Asokan, D. Arulkirubakaran, Effect of cryogenic cooling on machinability and surface quality of bio-degradable ZK60 Mg alloy, *Mater. Des.* 87 (2015) 1030-1036, <https://doi.org/10.1016/j.matdes.2015.08.099>.
- [25] E.M. Rubio, J.L. Valencia, A.J. Saá, D. Carou, Experimental study of the dry facing of magnesium pieces based on the surface roughness. *Int. J. Precis. Eng. Manuf.* 14 (2013) 995-1001, <https://doi.org/10.1007/s12541-013-0132-9>.
- [26] W. Akhtar, J. Sun, W. Chen, Effect of machining parameters on surface integrity in high speed milling of super alloy GH4169/Inconel 718, *Mater. Manuf. Process.* 31 (5) (2016) 620-627, <https://doi.org/10.1080/10426914.2014.994769>.
- [27] ISO I. 3685: Tool-Life Testing with Single-Point Turning Tools. International Organization for Standardization (ISO): Geneva, Switzerland, 1993.
- [28] M. Nurhaniza, M. Ariffin, F. Mustapha, B. Baharudin, Analyzing the Effect of Machining Parameters Setting to the Surface Roughness during End Milling of CFRP-Aluminium Composite Laminates, *Int. J. Manuf. Eng.* 2016 (1) (2016) 4680380, <https://doi.org/10.1155/2016/4680380>.
- [29] R. Kumar, P. Katyal, K. Kumar, Effect of end milling process parameters and corrosion behaviour of ZE41A magnesium alloy using Taguchi based GRA, *Biointerface Res. Appl. Chem.* 13 (3) (2023), <https://doi.org/10.33263/BRIAC133.214>.